Geomechanics and Engineering, *Vol. 17, No. 1 (2019) 109-118*
DOI: https://doi.org/10.12989/gae.2019.17.1.109

Numerical modeling on the stability of slope with foundation during rainfall

An T.P. Tran[1b], Ah-Ram Kim[2a] and Gye-Chun Cho[*1]

[1]*Department of Civil Engineering, Korea Advanced Institute for Science and Technology, 291 Daehak-ro, Yuseong-gu, Daejeon 305-701, Republic of Korea*
[2]*Department of Infrastructure Safety Research, Korean Institute of Civil Engineering and Building Technology (KICT), 283 Goyangdae-ro, Ilsanseo-gu, Goyang 10223, Republic of Korea*

(Received March 14, 2018, Revised November 16, 2018, Accepted December 17, 2018)

Abstract. The movement of soil along a slope during rainfall can cause serious economic damage and can jeopardize human life. Accordingly, predicting slope stability during rainfall is a major issue in geotechnical engineering. Due to rainwater penetrating the soil, the negative pore water pressure will decrease, in turn causing a loss of shear strength in the soil and ultimately slope failure. More seriously, many constructions such as houses and transmission towers built in/on slopes are at risk when the slopes fail. In this study, the numerical simulation using 2D finite difference program, which can solve a fully coupled hydromechanical problems, was used to evaluate the effects of soil properties, rainfall conditions, and the location of a foundation on the slope instability and slope failure mechanisms during rainfall. A slope with a transmission tower located in Namyangju, South Korea was analyzed in this study. The results showed that the correlation between permeability and rainfall intensity had an important role in changing the pore water pressure via controlling the infiltrated rainwater. The foundation of the transmission tower was stable during rainfall because the slope failure was estimated to occur at the toe of the slope, and did not go through the foundation.

Keywords: slope failure; safety factor; rainfall infiltration; pile displacement

1. Introduction

The movement of soil along slopes during rainfall can cause serious economic damage and jeopardize human life. In Korea, the typhoon season often extends through July, August, and September (Soh 2013). Table 1 shows typhoons that affected the Korean peninsula from 1999 to 2009 and accompanied extremely high rainfall intensity levels. For example, the Maemi typhoon on 12 September 2003 was the most destructive typhoon with wind speeds of 60 m/s and rainfall intensity greater than 50.8 mm/h, causing widespread damage from the Nakdong River basin to the port of Pusan and populated areas in the southeast region of the Korean peninsula (Ji and Julien 2005).

The extreme rainfall on 27 July 2011 in Seoul marked the highest rainfall intensity thus far on record. A peak rainfall intensity of 112.5 mm/h and cumulative rainfall of 306.5 mm over 16 hours caused a total of 33 debris flows at Mt. Umyeon, resulting in 16 fatalities and extensive damage to houses, roads, and other infrastructure (Jeong *et al.* 2015). In many cases, footings of structures such as retaining walls, power transmission towers are located on aslope surface (Varzaghani and Ghanbari 2014). Therefore, the mass movement of soil induced by heavy rainfall can also seriously impact the stability of the structures. In which, failure of a transmission tower causes an interruption in electricity and in turn leads to devastating economic losses as well as negative social consequences. Therefore, additional research should be carried out on the instability of foundations located on slopes during rainfall considering the soil characteristics in Korea.

Numerous studies have been performed on key factors such as the rainfall condition and soil properties influencing rainfall-induced slope failures. For the rainfall condition, intensity, duration, and antecedent condition are the important factors in terms of the stability of an unsaturated slope considering rainfall infiltration (Lee and Kim 2013, Tsaparas *et al.* 2002). For soil properties, soil type and infiltration characteristic are considerably influential factors on slope failures due to the decrease in the shear strength caused by a loss of suction (negative) pressure in unsaturated soils. In other words, coarse-grained soil and high infiltration rates lead to the development of positive pore pressures, and failure will be caused by seepage forces, whereas fine-grained soil that has low infiltration characteristics does not let rain water penetrate the ground (Collins and Znidarcic 2004). The hydraulic characteristics of soil greatly influence the formation and dissipation of pore pressure in slopes (Cai and Ugai 2004, Roy *et al.* 2009, Tsaparas *et al.* 2002)

The aim of this study is to investigate the stability of an unsaturated slope with pile foundations considering rainfall infiltration. A test site having a slope with a transmission tower located in Namyangju City in Korea was selected in

∗Corresponding author, Professor
E-mail: gyechun@kaist.edu
[a]Research Specialist
E-mail: kimahram@kict.re.kr
[b]Ph.D. Candidate
E-mail: sanga@kaist.ac.kr

http://www.techno-press.org/?journal=gae&subpage=7 ISSN: 2005-307X (Print), 2092-6219 (Online)

Table 1 Type of typhoon tracks that affected the Korean Peninsula from 1999 to 2009 (data after (Bureau 1999a, Bureau 1999b, Ji and Julien 2005, Jung 2015, Kim *et al.* 2006, McPherson and Stapler 1999, Padgett 2000, Padgett 2004, Padgett 2008, Pete and Engel 2002, Savage 2006)

Type	Characteristics	Typhoon	Year	Rainfall intensity (mm/h)
The Western sea	Moved northward in the West Sea and landed on the west coast	Neil Olga Ann Rammasun	1999 1999 1999 2002	8.3 25.0 04.0 15.5
	Passed along China and affected the Korean Peninsula	Bilis Kalmaegi	2000 2008	9.7 2.0
The Southern sea	The typhoon landed on the shore of southern coast	Saomai; Rusa Maemi Ewiniar; Nari	2000 2002 2003 2006 2007	4.1 36.3 50.8 10.8 24.5
The Eastern sea	Passed along the straits of Korea and went through the northern eastern sea area	Megi	2004	13.8
	Passed along Japan and affected the Korean Peninsula	Usagi	2007	4.2

this study. A fully coupled hydraulic-mechanical analysis was performed to evaluate the effects of rainfall conditions, soil properties (i.e., permeability), and pile foundations (i.e., position and spacing) on the failure mechanism of a transmission tower located on an unsaturated slope. Based on the analysis results, it can be concluded that the suggested numerical analysis using FLAC2D reasonably evaluated the stability of a slope with foundations during rainfall, and it is expected that the results of this study can be used to design foundations and a drainage system for slope stability.

2. Analysis method

2.1 Shear strength reduction method

The shear strength reduction method is a powerful tool for slope stability analysis. The factor of safety (FoS) of the slope can be easily calculated via reducing effective cohesion and tangent of effective friction angle in equal proportion (Tu *et al.* 2016).

Based on Bishop's effective stress (Bishop 1959) the shear strength (Eq. (1)) and the effective stress (Eq. (2)) are expressed as

$$\tau_{\max} = \sigma^b \tan\phi' + c' \quad (1)$$

where τ_{max} is the shear strength, ϕ' is the effective friction angle, c′ is the effective cohesion of the soil, and σ^b is the effective stress.

$$\sigma^b = (\sigma - u_a) + \chi(u_a - u_w) \quad (2)$$

where χ is a parameter with a value between zero and unity depending on soil type and the degree of saturation assuming that the pore water does not occupy the total pore volume (Cai and Ugai 2004), and u_a and u_w are air and water pressure, respectively.

The value of parameter χ can roughly be replaced by the degree of saturation or the relative degree of saturation as (Vanapalli *et al.* 1996),

$$\chi = \frac{S_w - S_r}{1 - S_r} \quad (3)$$

where S_w denotes the degree of water saturation and S_r is the degree of residual saturation.

From Eqs. (1)-(3), the yield criterion can be represented as follows

$$\tau_{\max} = (\sigma - u_a)\tan\phi' + \frac{S_w - S_r}{1 - S_r}(u_a - u_w)\tan\phi' + c' \quad (4)$$

For unsaturated soil, additional cohesion c_c by capillary pressure defined as u_c (= $u_a - u_w$) can be expressed as the second term in Eq. (4) as

$$\tau_{\max} = (\sigma - u_a)\tan\phi' + c_c + c' \quad (5)$$

To calculate the safety factor of an unsaturated slope using a shear strength reduction technique, a set of simulations is performed with the reduced shear strength parameters C^{trial} and ϕ^{trial} defined as follows

$$C^{trial} = \frac{1}{F^{trial}} C \quad (6)$$

$$\phi^{trial} = \left(\arctan \frac{1}{F^{trial}} \tan\phi \right) \quad (7)$$

where F^{trial} is the trial factor of safety.

The initial shear strength reduction F^{trial} is set to be sufficiently small to ensure the stability of the slope. F^{trial} is then increased incrementally until a failure occurs and that value is considered to be the factor of safety of the slope.

2.2 Rainfall infiltration model

Various empirical models and equations have been developed in order to determine the relationship between the soil suction and the volumetric water content in unsaturated soils (Brooks and Corey 1964, Fredlund and Xing 1994, Gardner 1958, McKee and Bumb 1987, van Genuchten 1980). Two models, suggested by Fredlund and Xing (1994) and van Genuchten (1980), have been used by many researchers (Kim *et al.* 2004, Lee and Kim 2013, Stormont and Anderson 1999, Yang *et al.* 2004). In this study, van Genuchten equation, which is available model in FLAC, was used.

The set of closed-form equations formulated by van Genuchten (1980), based on the Mualem capillary model

(Mualem 1976a, b, van Genuchten and Nielsen 1985), is used to represent the hydraulic characteristics of unsaturated soils as follows

$$S_e = \frac{S_w - S_r}{1 - S_r} = \left[\frac{1}{1+(\alpha\varphi)^n}\right]^m \tag{8}$$

$$K(\theta) = K_s K_r = K_s S_e^{1/2}\left[1 - \left(1 - S_e^{1/m}\right)^m\right]^2 \tag{9}$$

$$u_c = u_0\left[S_e^{-1/a} - 1\right]^{1-a} \tag{10}$$

where S_e denotes the effective saturation (i.e., χ); α, n, and m (cf., m is defined as $1 - 1/n$) are van Genuchten parameters; K_s and K_r are the saturated and relative permeability, respectively; and u_0 is the reference capillary pressure.

2.3 Pile foundation of transmission tower

A row of equally spaced piles was simulated as plane-strain symmetry in FLAC2D. Actual forces and moments in the spaced pile foundations were evaluated at each simulation step. The shear and normal stiffness are important parameters to consider the shear and normal behavior of interaction between the pile and soil. The shear behavior of the pile-grid (i.e., soil) interaction is represented as a spring-slider system in which the relative displacement between the piles node and the grid is described numerically by the coupling spring shear stiffness. Similarly, the relative normal displacement between the pile nodes and the grid is described numerically by the coupling spring normal stiffness. Based on the experimental studies and the simulation results, the shear and normal stiffness are approximately similar (Kwon *et al.* 2013). A good rule of thumb is to set k_n and k_s to ten times the equivalent stiffness of the stiffest neighboring zone, and the apparent stiffness of a zone, k_z in the normal direction can be expressed as follows (Itasca 2011)

$$k_z = \max\left[\frac{\left(K + \frac{4}{3}G\right)}{\Delta Z_{\min}}\right] \tag{11}$$

$$k_n = k_s = 10.k_z \tag{12}$$

where K and G are the bulk and shear modulus of soil, respectively, and ΔZ_{min} is the smallest width of an adjoining zone in the normal direction.

3. Numerical analysis

A numerical simulation was developed to evaluate the stability of a slope and a pile foundation during a rainstorm and to analyze the slope-failure characteristics depending on the pile properties such as position (i.e., location) and spacing. In order to simulate the matric

Table 2 Position and spacing of pile considered in this study

D [m]	s [m]	s/D	L_x [m]
	9	2.25	44
	10	2.50	44
4	11	2.75	20, 25, 36, 44
	12	3.00	44
	13	3.25	44

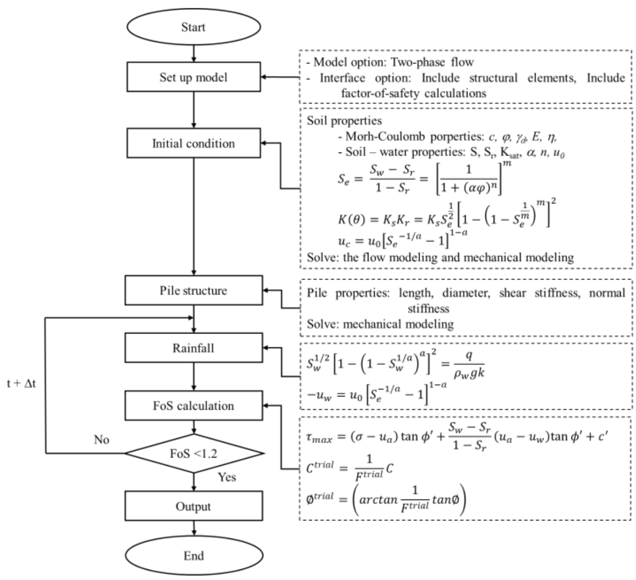

Fig. 1 Algorithm of numerical analysis on slope stability with pile foundation during rainfall

suction distribution in an unsaturated slope, a two-phase flow (i.e., gas and water flow) was used in the numerical modeling.

In this study, there is no horizontal displacement through the lateral mesh boundaries and no displacement along the bottom mesh boundary of the slope. As rainfall intensities are applied along the slope (i.e., rainwater-infiltrating boundary), the flow modeling with FLAC is done in parallel with the mechanical modeling. At the rainfall-infiltrating boundary, the pore air pressure is ambient (i.e., zero)

Fig. 1 shows the overall algorithm of the simulation to assess the three main points of interest of this study:

• Effects of the pile existence

L_x is defined as the distance from the left boundary of the slope to the first pile position, and *s/D* is the ratio of the pile spacing to the diameter of the pile (Khari *et al.* 2013, Lee *et al.* 1995, Li *et al.* 2011, Won *et al.* 2005). In order to estimate the effects of the position and spacing pile foundation on the FoS and the failure mechanism, different values of L_x and *s/D* were considered (Table 2).

• Effects of rainfall on the slope stability

The effects of rainwater on rainfall-induced slope failure were emphasized by considering the ratio of the rainfall condition (r) to the hydraulic permeability (k) (i.e., r/k). In this study, r/k ratios of 0.5, 1, 2, 4, and 10 considering permeability of 1.08 cm/h were used to investigate the effects of the rainfall intensity and duration on the slope instability. The failure mechanism of the slope at a certain rainfall intensity could thus be determined. In addition, the

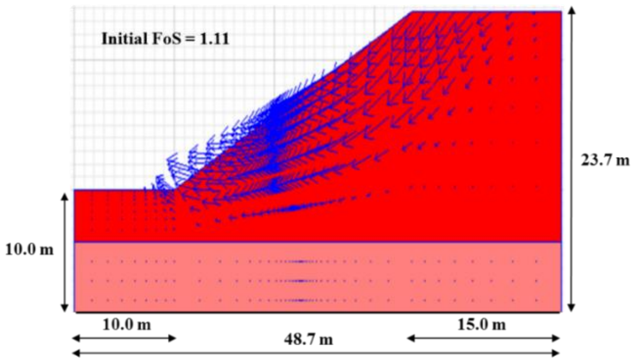

(a) Slope geometry and initial slope safety

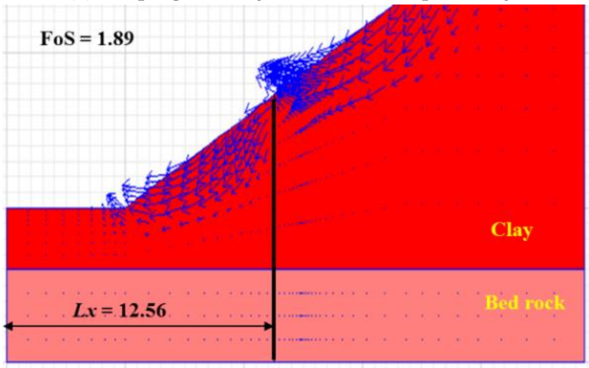

(b) Verified result by the FLAC code in this study

Fig. 2 Verification of piled slope simulation

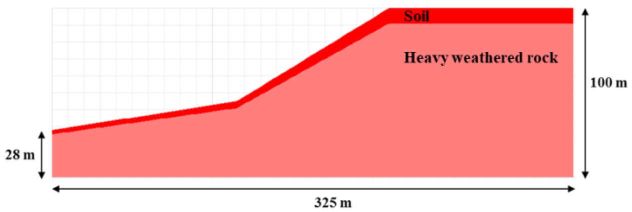

Fig. 3 Geometry of Mt. Umyeon (data from Jeong *et al.* 2014)

Table 3 Properties of Mt. Umyeon soils

Properties			Soil	Weathered rock
Dry density		[g/cm^3]	1800	1848
Friction angel		[°]	26.5	26.5
Cohesion		[Pa]	0	8000
Saturated permeability		[cm/h]	2.88	0.72
Saturation			0.6	0.72
Residual saturation			0.18	0.18
van Genuchten parameter	α	[m^{-1}]	0.88	0.88
	n		0.25	0.25

permeability values were changed from 0.108 cm/h to 10.8 cm/h to estimate the effect of the level of hydraulic permeability on the stability of the slope during rainfall.

• Effects of rainfall on the pile foundation stability

In order to determine the effects of rainfall on the foundation stability, the displacement of the pile was obtained with the rainfall time.

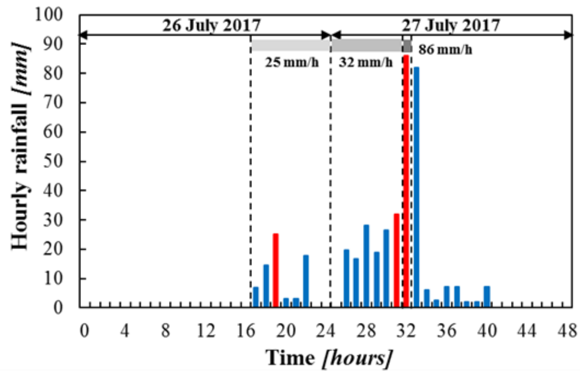

Fig. 4 Rainfall on Mt. Umyeon during 26 and 27 July 2011 (data from Jeong *et al.* 2014)

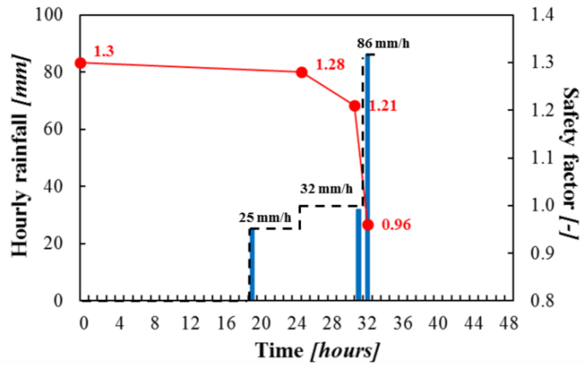

Fig. 5 Decrease of the FoS during 16 hours of rainfall

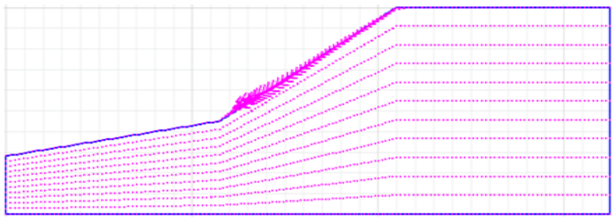

(a) Failure slope from simulation results

(b) Landslide track on Mt. Umyeon (Jeong *et al.* 2014)

Fig. 6 Slope failure along Mt. Umyeon after 16 hours of rainfall

4. Verification of simulation

In order to verify the numerical analysis method used in this study, two cases of pile and rainfall simulations were carried out. First, the pile-installed slope that is analyzed using FLAC2D (Li *et al.* 2011) was used to verify the

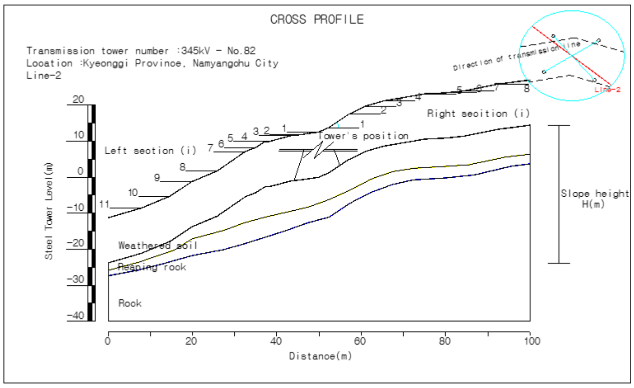

(a) Failure slope from simulation results

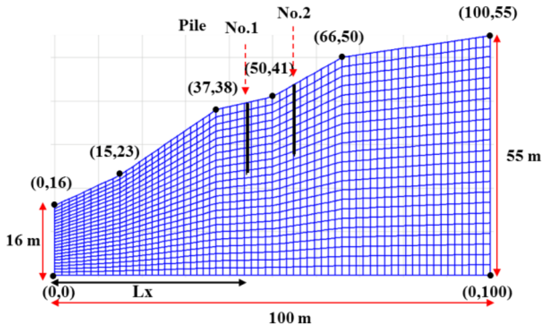

(b) Landslide track on Mt. Umyeon (Jeong *et al.* 2014)

Fig. 7 Cross-section and geometry of the target slope

Table 4 Properties of weathered soil and pile foundation in targeted slope

Properties				
Soil	Unit weight	$\gamma_{w(s)}$	[t/m^3]	1.7
	Effective cohesion	c'	[kPa]	0.0
	Effective friction angle	ϕ'	[°]	31.7
	Young's modulus	E_s	[MPa]	84.0
	Poisson ratio	η	[-]	0.3
	Initial saturation	S	[-]	0.5
	Residual saturation	S_r	[-]	0.1
	Saturated permeability	K_{sat}	[cm/h]	1.1
van Genuchten parameters	α		[m^{-1}]	1.9
	n		[-]	1.5
Concrete pile	Unit weight	$\gamma_{w(c)}$	[t/m^3]	2.4
	Elastic modulus	E_c	[Pa]	34.0
	Diameter	D	[m]	4.0
	Length	l	[m]	16.5
Pile-soil interface	Shear stiffness	K_s	[GPa/m]	1.2
	Normal stiffness	K_n	[GPa/m]	1.2

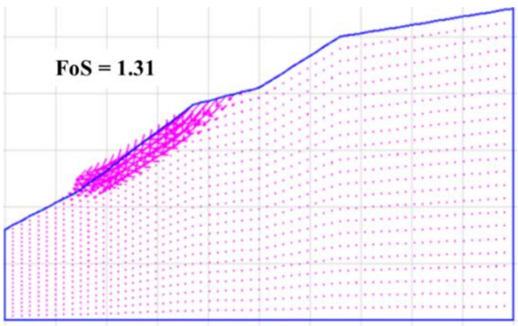

Fig. 8 Initial FoS and failure curve of the natural slope

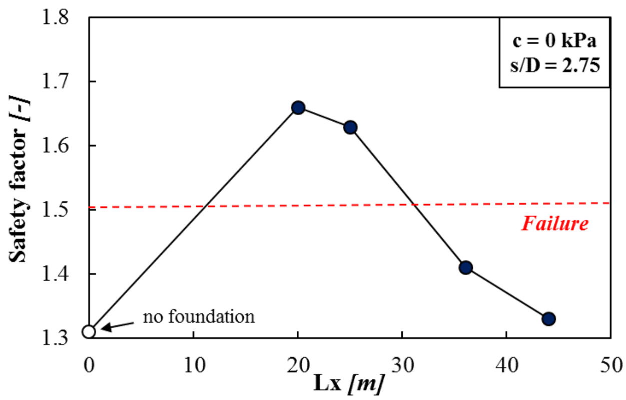

(a) Effect of the pile position on the FoS

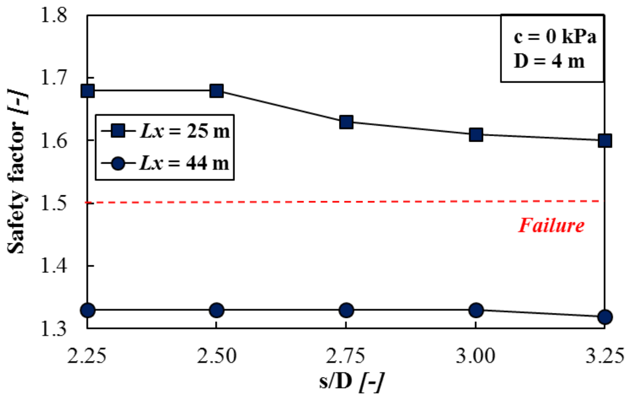

(b) Effect of pile spacing on the FoS

Fig. 9 Effect of pile foundation on the FoS before rainfall

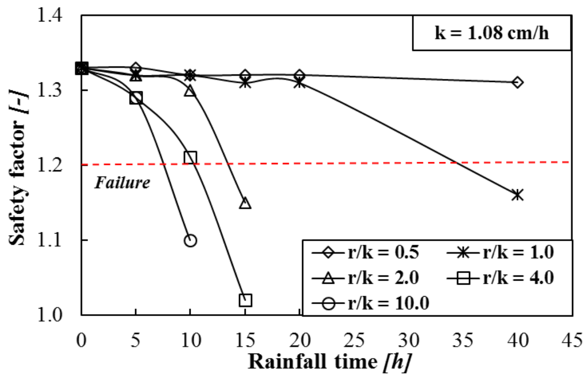

(a) Safety factors of various rainfall intensities with rainfall time

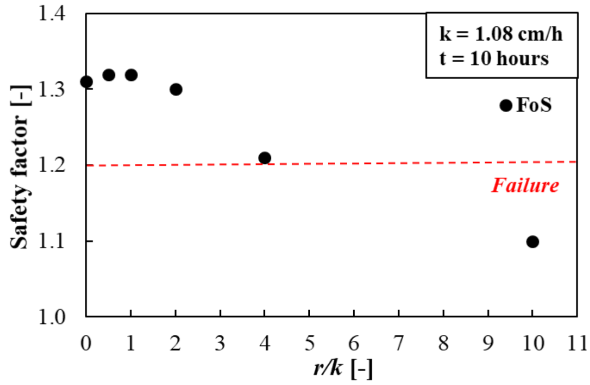

(b) Safety factors after 10 hours of varying rainfall intensities

Fig. 10 Effect of rainfall intensities on slope stability levels

Detailed information on the pile and soil properties can be found in their paper (Li *et al.* 2011). The initial FoS of a natural slope is 1.11 with soil movement, as shown in Fig. 2(a). A pile was installed at Lx = 12.56, and the obtained FoS and failure mechanism (Fig. 2(b)) were quite similar to the results obtained by Li *et al*. (2011).

Second, a real case of a landslide at Mt. Umyeon in Korea was simulated to verify the numerical code on the slope instability induced by heavy rainfall. Mt. Umyeon comprises of steep hills, gullies and valleys and is topographically characterized by pre-Cambrian metamorphic gneiss associated with the Gyeonggi massif (Kim and Jeong 2017). Referring to studies of Jeong *et al.* (2014) and Jeong *et al.* (2015), the chosen properties of soils at the initial condition are summarized in Table 3. The geometry of Mt. Umyeon and the amount of rainfall per hour are shown in Figs. 3 and 4, respectively. In fact, the highest rainfall intensity on 26 July 2011 was 25 mm/h, and on the next day, a major rainfall of 86 mm/h occurred right after a rainfall of 32 mm/h.

Based on the hourly rainfall data for 26 and 27 July 2011 (Fig. 4), three rainfall patterns were used in this study. The slope was subjected to a rainfall of 25 mm/h for nine hours on 26 July. A second rainfall with intensity of 32 mm/h occurred for six hours before a major rainfall with intensity of 86 mm/h lasting 1 hour, which caused slope to failure (FoS < 1.2) on 27 July 2011. Given that the high effective cohesion used in the simulation of a shallow failure can cause an overestimated value of FoS (Fell *et al.* 2005), the effective cohesions of soil and rock are assigned values of zero and 8,000 Pa, respectively.

Fig. 5 shows the reduction of the FoS after the first 16 hours of rainfall. The FoS gradually decreased during antecedent rainfalls, and a significant decrease in the FoS was caused by a major rainfall (i.e., 86 mm/h) with a FoS of 0.96. The slope failure curve from the simulation results (Fig. 6(a)) is considerably similar to the configuration of the real landslide on Mt. Umyeon, as shown in Fig. 6(b).

5. Site of interest

A slope in Namyangju City, Gyeonggi Province, South Korea was targeted the application of the developed model. A representative cross-section and the geometry of the target slope are shown in Figs. 7(a) ad 7(b), respectively. The geometry of the targeted slope is a height of 39 m and a width of 100 m. The geotechnical and soil-water characteristic curve (SWCC) properties of the weathered soil provided by the Korea Electric Power Corporation (KEPCO) are summarized in Table 4.

Four pile foundations were distributed and perpendicularly located at 44 m and 55 m from the toe of the slope, as shown in Fig. 7. The pile foundation has a length of 16.5 m and a diameter of 4 m, and the properties of the piles are summarized in Table 4. The shear and normal stiffness of the soil-pile interface were determined by Eqs. (11)-(12). The unit weight and the elastic modulus of the pile were assumed using the properties of general concrete. Other properties were provided by KEPCO. Based on the field survey, the ground water level was not observed at the target slope.

6. Results and analysis

6.1 Effects of piles on the slope stability before rainfall

The simulation results show that the installation of a pile foundation increases the FoS of the slope, which depends on the position and spacing of the piles within the slope (Figs. 8 and 9). As shown in Fig. 8, the FoS of the natural slope is about 1.31. After the pile foundations were installed at the planned position (L_x = 44 m and 55 m), the slope failure was predicted to occur at the front of the foundation (L_x = 44 m). It can be seen from Fig. 9(a), there is no significant effect of the pile foundation on the improvement of the slope stability (FoS = 1.33). Meanwhile, the maximum FoS is obtained when the foundation was located at L_x = 20 m. When the pile was located farther away from the toe of the slope, lower FoS values are obtained. The pile spacing does not significantly affect the FoS value, as shown in Fig. 9(b).

6.2 Effect of rainfall intensity and hydraulic permeability on the slope stability

The higher the *r/k* ratio becomes, the faster the FoS decreases (Fig. 10(a)). A lower rainfall intensity level (*r/k* = 0.5) with a given permeability value (*k* = 1.08 cm/h) does not cause a significant decrease in the FoS, even after 40 hours of rainfall, as shown in Fig. 10(a). On the contrary, the FoS abruptly drops after 10 hours with a higher rainfall intensity (*r/k* = 10) due to the change in the pore water pressure. In other words, at a lower level of rainfall intensity, the amount of water that infiltrated into the soil does not considerably decrease the negative pore water pressure, and the FoS therefore decreases slowly. Under an extremely heavy rainfall, the rain water penetrates faster and the soil is then saturated in a relatively short time. For instance, Fig. 10(b) shows the FoS after the first 10 hours of rainfall under varying rainfall intensities. High rainfall intensities cause the value of the negative pore pressure and saturation to become almost zero and one, respectively, and consequently the FoS will be in the failure zone. The detail changes in matric suction and water saturation after 10 hours of rainfall for different rainfall intensities are shown in Figs. 11 and 12.

The effect of saturated permeability on the FoS under a given rainfall condition is shown in Fig. 13(a). For the lowest permeability (i.e., 0.108 cm/h), rainwater cannot easily penetrate into the soil. Thus, the decrease in the negative pore pressure is too small to cause a considerable decrease in the FoS. Similarly, the highest permeability (i.e., 10.8 cm/h) also does not cause a rapid FoS decrease. Due to the small amount of rainwater, which quickly distributed within the soil, the decrease in the pore pressure at the surface occurs gradually, leading to a gentle decrease in the FoS during rainfall. The most rapid drop in the FoS can be seen when the soil has a moderate permeability of 1.08 cm/h. The soil movement after 20 hours of rainfall is shown in Fig. 13(b). The results indicate that the correlation between permeability and rainfall intensity plays an important role in the change of pore water pressure via controlling infiltrated rainwater.

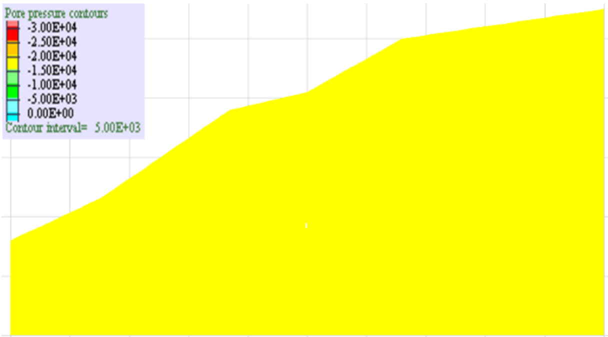

(a) Before rainfall

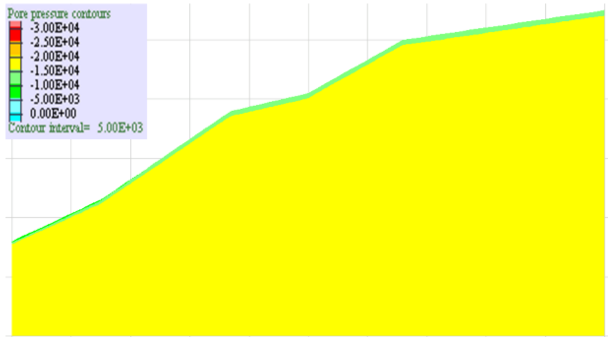

(b) After 10 hours of rainfall with the *r*/*k* ratio of 0.5

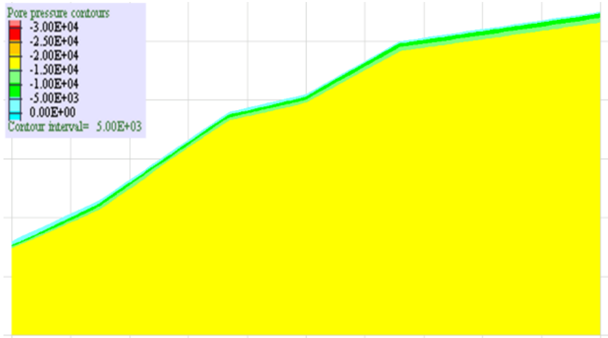

(c) After 10 hours of rainfall with the *r*/*k* ratio of 2

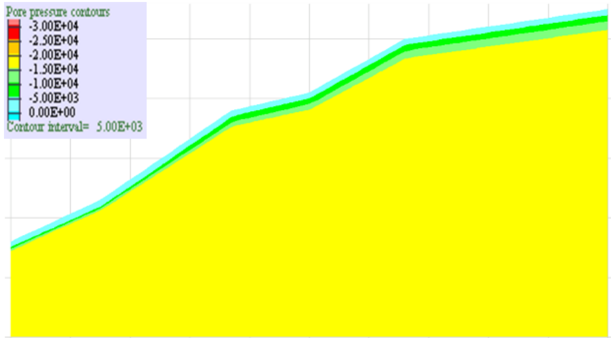

(d) After 10 hours of rainfall with the *r*/*k* ratio of 10

Fig. 11 Distribution of matric suction (a) before rainfall, and after 10 hours of rainfall (b) with the *r*/*k* ratio of 0.5, (c) with the *r*/*k* ratio of 2 and (d) with the *r*/*k* ratio of 10

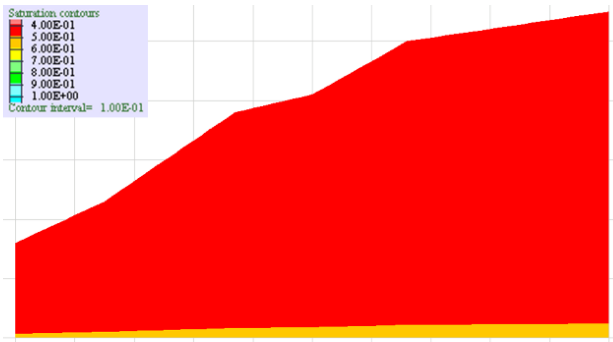

(a) Before rainfall

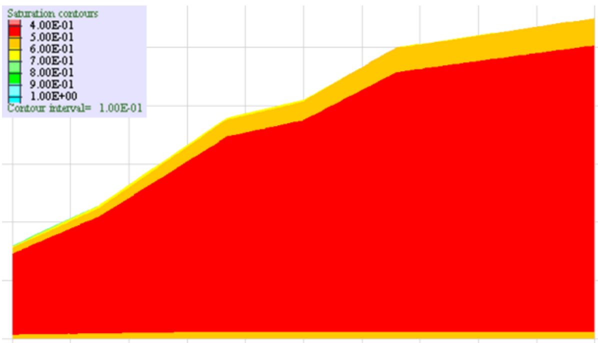

(b) After 10 hours of rainfall with the *r*/*k* ratio of 0.5

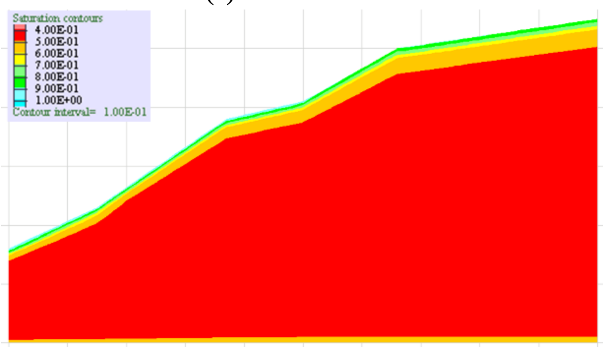

(c) After 10 hours of rainfall with the *r*/*k* ratio of 2

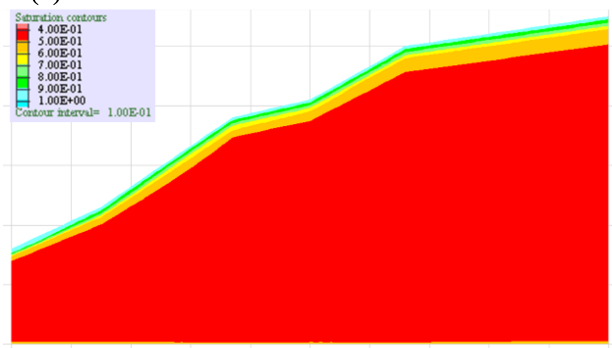

(d) After 10 hours of rainfall with the *r*/*k* ratio of 10

Fig. 12 Distribution of water saturation (a) before rainfall, and after 10 hours of rainfall (b) with the *r*/*k* ratio of 0.5, (c) with the *r*/*k* ratio of 2 and (d) with the *r*/*k* ratio of 10

6.3 Effect of rainwater on the pile foundation stability

Fig. 14 presents the structural displacement of the pile foundation under different rainfall intensities with the given permeability of 1.08 cm/h. The displacement of the foundation gradually increases during rainfall. The maximum displacements are obtained as the slope failure appears. However, the displacement values are very small

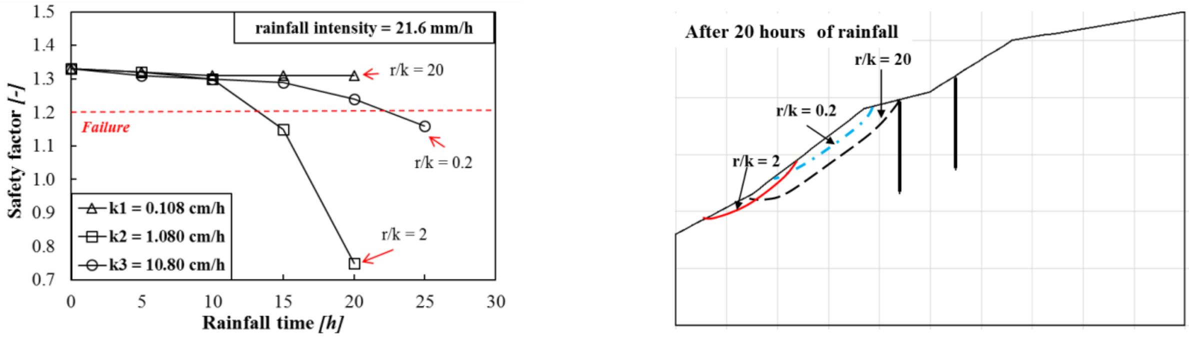

(a) Reduction in FoS with rainfall time (b) Failure curve after 20 hours of rainfall

Fig. 13 Effects of permeability under a given rainfall

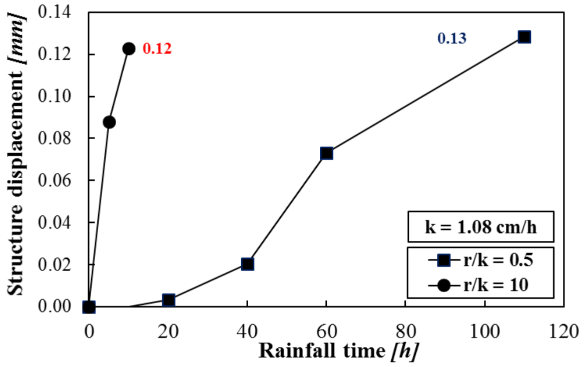

Fig. 14 Effect of rainfall on foundation displacement

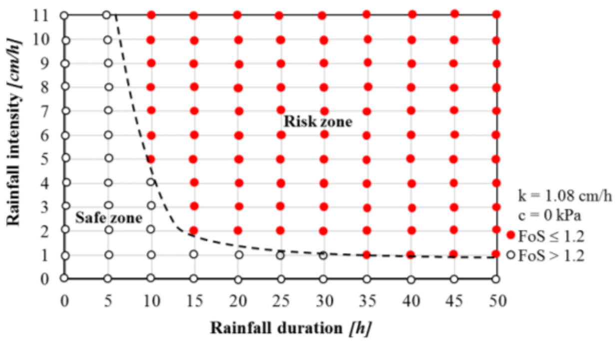

Fig. 15 Initial FoS and failure curve of the natural slope

(about 1 mm) under a heavy rainfall condition (i.e., r/k = 10), indicating that the rainfall does not strongly affect the stability of the foundation. This is because the predicted shallow slope failure does not pass through the foundation.

7. Discussion

As mentioned in the previous sections, the existence of the pile foundation have only a small effect on the stability of the target slope, because the position of the foundation does not significantly improve the FoS of the slope, and the predicted failure surface does not go through the foundation. The results also show that the slope stability is considerably influenced by the rainfall conditions and soil properties of the slope compared to the pile foundation. The relationships among the three parameters of the permeability, the rainfall condition, and the pore pressure are the major factors affecting rainfall-induced slope failures. The simulation results imply that the relationship between the permeability and rainfall conditions determines the seepage behavior and consequent distribution of the pore water pressure in the unsaturated soil.

Using FLAC2D code, the simulation results provide a FoS database of the targeted slope with rainfall intensity and duration. Fig. 15 indicates the relationships of the slope stability versus rainfall intensity and rainfall duration. The white dots denote the FoSs that are larger than 1.2, while red dots represent the FoS that are less than or equal to 1.2. The larger rainfall intensity is the faster slope failure takes place. The slope does not fail when the rainfall duration is less than a certain value due to its quite large hydraulic conductivity. As shown in Fig. 15, the numerical modelling data can be divided into two zones: a safe zone that contains the white dots and a risk zone that contains the red dots. The dash curve is the envelope curve of instability for the target slope. Based on the FoS chart, the stability of the slope can be evaluated under a given rainfall condition.

8. Conclusions

In this study, a numerical modeling was conducted to investigate the stability of a pile foundation and a slope during rainfall. A typical slope with a transmission tower in Namyangju, Korea was selected for this study. The ground water level was not tracked in the target slope area; and therefore shallow slope failures are the main types of failure that occur during rainfall. The numerical modelling showed that it is possible to use FLAC2D to predict the critical rainfall intensity and duration, under which the slope and/or foundation failure take place.

Regarding the improvement in the FoS, the optimum position of the pile system within the slope target is at the toe area of the slope (L_x = 20 m). The predicted shallow failure does not pass through the foundation; therefore, there is no effect on the foundation instability due to either movement of the soil along the slope or the seepage force within the slope.

The effects of the rainfall intensity level strongly depend on the permeability of the soil. With lower permeability, the pore pressure does not significantly change during rainfall, which is in good agreement with the findings by Tsaparas *et al.* (2002). However, it is highlighted that the correlation between permeability and rainfall intensity plays an important role in controlling the amount of water that penetrates into soil, leading to a change in negative pore pressure.

This study provides a database on the stability of the target slope during rainfall, which can be useful reference data for geotechnical engineers to estimate the slope instability under a given rainfall and to design and locate structures and/or drainage systems. In further studies to obtain the failure area more accurately, 3D model simulations should be conducted.

Acknowledgements

This research has supported by a grant (18AWMP-B114119-03) from the Water Management Research Program funded by the Ministry of Land, Infrastructure, and Transport (MOLIT) of the Korean Government and supported by the National Research Foundation of Korea (NRF) grant funded by the Korea government (MSIT) (No. 2018R1CB6008417). The first author was supported by the third stage of the Brain Korea 21 Plus Project (21A20132000003) through the National Research Foundation (NRF) funded by the Ministry of Education of Korea.

References

Bishop, A.W. (1959), “The principle of effective stress”, Teknisk ukeblad, **39**, 859-863.

Brooks, R.H. and Corey, A.T. (1964), “Hydraulic properties of porous media and their relation to drainage design”, *Trans. ASAE*, **7**(1), 26-0028.

Bureau, W. (1999a), *Weekly Weather and Crop Bulletin (WAOB)*, United States Department of Agriculture, Economics, Statistics and Market Information System, **86**(32), 1-32.

Bureau, W. (1999b), *Weekly Weather and Crop Bulletin (WAOB)*, United States Department of Agriculture, Economics, Statistics and Market Information System, **86**(39), 1-24.

Cai, F. and Ugai, K. (2004), “Numerical analysis of rainfall effects on slope stability”, *Int. J. Geomech*., **4**(2), 69-78.

Collins, B.D. and Znidarcic, D. (2004), “Stability analyses of rainfall induced landslides”, *J. Geotech. Geoenviron*, **130**(4), 362-372.

Fell, R., MacGregor, P., Stapledon, D. and Bell, G. (2005), *Geotechnical Engineering of Dams*, CRC Press.

Fredlund, D.G. and Xing, A. (1994), “Equations for the soil-water characteristic curve”, *Can. Geotech. J*., **31**(4), 521-532.

Gardner, W. (1958), “Some steady-state solutions of the unsaturated moisture flow equation with application to evaporation from a water table”, *Soil Sci*., **85**(4), 228-232.

Itasca (2011), *Fast Lagrangian Analysis of Continua*, version 7.0, Itasca Consulting Group.

Jeong, S., Kim, J., Kim, Y. and Bae, D. (2014), “Susceptibility assessment of landslides under extreme-rainfall events using hydro-geotechnical model; A case study of Umyeonsan (Mt.), Korea”, *Nat. Hazards Earth Syst. Sci. Discuss*., **2**(8), 5575-5601.

Jeong, S., Kim, Y., Lee, J.K. and Kim, J. (2015), “The 27 July 2011 debris flows at Umyeonsan, Seoul, Korea”, *Landslides*, **12**(4), 799-813.

Ji, U. and Julien, P. (2005), “Typhoon Maemi and impacts on lower Nakdong River, South Korea”, *Hydrology Days*, 103-110.

Jung, W.S. (2015), “An estimation of extreme wind speed of typhoon affecting the damage of public and industrial facilities”, *J. Environ. Sci. Int*., **24**(9), 1199-1210.

Khari, M., Kassim, K.A. and Adnan, A. (2013), “An experimental study on pile spacing effects under lateral loading in sand”, *Sci. World J*.

Kim, J., Jeong, S., Park, S. and Sharma, J. (2004), “Influence of rainfall-induced wetting on the stability of slopes in weathered soils”, *Eng. Geol*., **75**(3), 251-262.

Kim, N., Won, Y. and Chung, I. (2006), “The scale of typhoon RUSA”, *Hydrol. Earth Syst. Sci*., **3**(5), 3147-3182.

Kim, Y. and Jeong, S. (2017), “Modeling of shallow landslides in an unsaturated soil slope using a coupled model”, *Geomech. Eng*., **13**(2), 353-370.

Kwon, S., Kim, M., and Choi, J. (2013), “3D dynamic numerical modeling for soil-pile-structure interaction in centrifuge tests”, *Proceedings of the 18th International Conference on Soil Mechanics and Geotechnical Engineering*, Paris, France, September.

Lee, C., Hull, T. and Poulos, H. (1995), “Simplified pile-slope stability analysis”, *Comput. Geotech*., **17**(1), 1-16.

Lee, J.S. and Kim, Y.T. (2013), “Infiltration and stability analysis of weathered granite slope considering rainfall patterns”, *J. Korean Soc. Hazard Mitig*., **13**(5), 83-91.

Li, X., He, S., Luo, Y. and Wu, Y. (2011), “Numerical studies of the position of piles in slope stabilization”, *Geomech. Geoeng*., **6**(3), 209-215.

McKee, C. and Bumb, A. (1987), “Flow-testing coalbed methane production wells in the presence of water and gas”, *SPE Form. Eval*., **2**(4), 599-608.

McPherson, T. and Stapler, W. (1999), “1999 Annual Tropical Cyclone Report”, DTIC Document, Naval Pacific Meteorology and Oceanography Center, Joint Typhoon Warning Center, Pear Harbor, Hawaii, U.S.A..

Mualem, Y. (1976a), “A new model for predicting the hydraulic conductivity of unsaturated porous media”, *Water Resour. Res*., **12**(3), 513-522.

Mualem, Y. (1976b), “Hysteretical models for prediction of the hydraulic conductivity of unsaturated porous media”, *Water Resour. Res*., **12**(6), 1248-1254.

Padgett, G. (2000), Monthly global tropical cyclone summary August 2000, <http://australiasevereweather.com/cyclones/2001/summ0008.htm>.

Padgett, G. (2004), Monthly global tropical cyclone summary August 2004, <http://australiasevereweather.com/cyclones/2005/summ0408.htm>. (Octorber 12, 2016).

Padgett, G. (2008), Monthly tropical weather summary for September 2007, <http://www.typhoon2000.ph/garyp_mgtcs/sep07sum.txt>.

Pete, F. and Engel, G. (2002), “2002 Annual tropical cyclone report”, US Naval Oceanography Command Center.

Roy, D., Chiranjeevi, K., Singh, R. and Baidya, D.K. (2009), “Rainfall induced instability of mechanically stabilized earth embankments”, *Geomech. Eng*., **1**(3), 193-204.

Savage, S. (2006), Typhoon leaves at least six dead in South Korea, RedOrbit, <http://www.redorbit.com/news/science/566417/typhoon_leaves_at_least_six_dead_in_south_korea/?source=r_science>.

Soh, C.T. (2013), *Korea: A geomedical monograph of the Republic of Korea*, Springer Science & Business Media.

Stormont, J.C. and Anderson, C.E. (1999), “Capillary barrier effect from underlying coarser soil layer”, *J. Geotech. Geoenviron*., **125**(8), 641-648.

Tsaparas, I., Rahardjo, H., Toll, D.G. and Leong, E.C. (2002), “Controlling parameters for rainfall-induced landslides”,

Comput. *Geotech*., **29**(1), 1-27.
Tu, Y., Zhong, Z., Luo, W., Liu, X., and Wang, S. (2016), "A modified shear strength reduction finite element method for soil slope under wetting-drying cycles", *Geomech*. *Eng*., **11**(6), 739-756.
van Genuchten, M.T. (1980), "A closed-form equation for predicting the hydraulic conductivity of unsaturated soils" *Soil Sci*. *Soc*. *Am*. *J*., **44**(5), 892-898.
van Genuchten, M.T. and Nielsen, D. (1985), "On describing and predicting the hydraulic properties of unsaturated soils", *Ann*. *Geophys*., **3**(5), 615-628.
Vanapalli, S., Fredlund, D., Pufahl, D. and Clifton, A. (1996), "Model for the prediction of shear strength with respect to soil suction", *Can*. *Geotech*. *J*., **33**(3), 379-392.
Varzaghani, M.I. and Ghanbari, A. (2014), "A new analytical model to determine dynamic displacement of foundations adjacent to slope", *Geomech*. *Eng*., **6**(6), 561-575.
Won, J., You, K., Jeong, S. and Kim, S. (2005), "Coupled effects in stability analysis of pile-slope systems", *Comput*. *Geotech*., **32**(4), 304-315.
Yang, H., Rahardjo, H., Leong, E.C. and Fredlund, D.G. (2004), "Factors affecting drying and wetting soil-water characteristic curves of sandy soils", *Can*. *Geotech*. *J*., **41**(5), 908-920.

CC